*Organometallics* **2007,** *26,* 2149−2156

# Bimetallic Complexes of Metallacyclopentynes: *cis* versus *trans* and Planarity versus Nonplanarity

Marc A. Bach,[†] Pattiyil Parameswaran,[‡] Eluvathingal D. Jemmis,*[,‡] and Uwe Rosenthal[†]

*Leibniz-Institut für Katalyse e.V. an der Universität Rostock, Albert-Einstein-Strasse, 29a Rostock, Germany, and Department of Inorganic and Physical Chemistry, Indian Institute of Science, Bangalore -560012, India*

*Received November 8, 2006*

Density functional theory calculations show that the $Cp_2M$ in *cis*-dimetallabicycles of metallacyclopentynes, $Cp_2M[\mu\text{-}(\eta^4{:}\eta^2\text{-}H_2C_4H_2)]M'L_2$ (M = Ti, Zr and M′ = Ti, Zr), deviates from the C4 plane. Both the metal fragments deviate from the C4 plane in the nickel complexes of metallacyclopentynes (**3Ti-Ni** and **3Zr-Ni**). The nonplanarity of $Ni(PH_3)_2$ from the C4 plane reduces the antibonding interaction between nickel orbitals and the $\pi$-MO at the C2−C3 bond, whereas that of the $Cp_2M$ acts mainly to reduce the antibonding interaction between C1 and C2. The energetics of the isodesmic equations show that the nickel complexes **3Ti-Ni** and **3Zr-Ni** are more stable than the homodimetallabicycles, **3Zr-Zr** and **3Ti-Ti**. The electron deficiency on the *cis*-homodimetallabicycles due to the vacant d-orbital on $\eta^2$-M′ can be decreased by accepting electrons from a Lewis base or by flipping into *trans* geometry. This is reflected in the experimental realization of *cis*-$Cp_2Zr[\mu\text{-}(\eta^4{:}\eta^2\text{-}H_2C_4H_2)]ZrCp_2(PMe_3)$ and the *trans* geometry for $Cp_2Ti[\mu\text{-}(\eta^3{:}\eta^3\text{-}H_2C_4H_2)]TiCp_2$ and $Cp_2Zr[\mu\text{-}(\eta^3{:}\eta^3\text{-}H_2C_4H_2)]ZrCp_2$.

## Introduction

The chemistry of unstable 14-electron titanocene “$Cp_2Ti$”[1] and zirconocene “$Cp_2Zr$”[2] fragments has been playing a vital role in structural and catalytic chemistry. These metallocenes are important in stoichiometric C−C coupling reactions of unsaturated molecules such as alkynes, olefins, or groups like acetylides and vinylidenes.[3] The carbene-type frontier orbitals of $Cp_2M$ (M = Zr, Ti) help in the reaction with unsaturated compounds to form several metallacycles. Two of these unusual metallacycles, viz., the metallacyclocumulenes and the metallacyclopentynes, show similar bonding patterns, despite the two formal $sp^3$ carbons in the latter.[4] The central unsaturated C−C bond of metallacyclocumulenes and metallacyclopentynes is able to coordinate to other metal fragments to form binuclear complexes.[5] These bimetallic complexes have either *cis*- or *trans*-butatriene (**3M-M′** or **5M-M′**) or butadiyne (**4M-M′** or **6M-M′**) ligands between two metal centers (Scheme 1). The butatriene or butadiyne skeleton and the metals are usually in the same plane. The structure and bonding of the planar bimetallic complexes of butadiyne ligands have been studied in detail.[6]

### Scheme 1

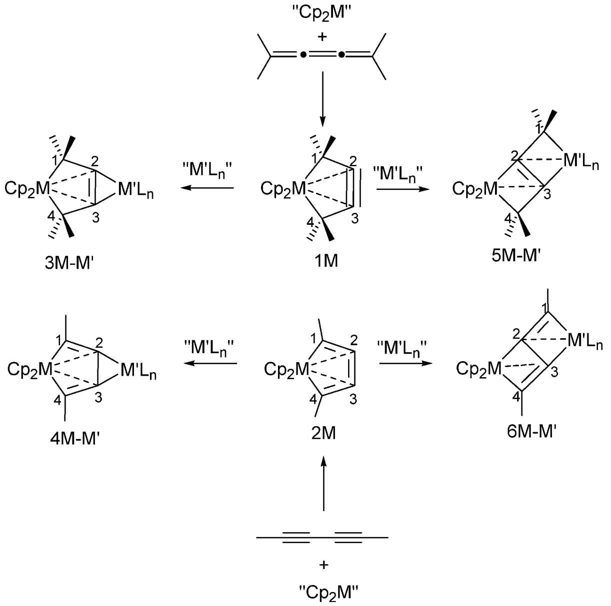

We have recently reported the synthesis of binuclear complexes $Cp_2Zr[\mu\text{-}(\eta^4{:}\eta^2\text{-}H_2C_4H_2)]NiL_2$ (L = $PPh_3$, $PCy_3$)[5b] (**3M-M′**, M = Zr and M′ = Ni, Scheme 1). The $ZrC_4Ni$ unit in these complexes is not planar (Figure 1). The deviation of $NiL_2$ from the C4 plane ($\theta$) is 16.9° for L = $PPh_3$ and 5.7° for L = $PCy_3$. Similarly the $Cp_2Zr$ deviates from the C4 plane ($\phi$) by 16.5° for L = $PPh_3$ and 12.3° for L = $PCy_3$. On the other hand Suzuki

---

* Corresponding author. Fax: +91-80-2360-1552. E-mail: jemmis@ipc.iisc.ernet.in.

[†] Leibniz-Institut für Katalyse e.V. an der Universität Rostock.

[‡] Indian Institute of Science.

(1) Beckhaus, R. In *Metallocenes−Synthesis, Reactivity, Applications*; Togni, A., Halterman, R. L., Eds.; Wiley-VCH: Weinheim, 1998; Vol. 1, Chapter 4, p 153, and references therein.

(2) Negishi, E.; Montchamp, J.-L. In *Metallocenes−Synthesis, Reactivity, Applications*; Togni, A., Halterman, R. L., Eds.; Wiley-VCH: Weinheim, 1998; Vol. 1, Chapter 5, p 241, and references therein.

(3) Rosenthal, U. *Angew. Chem.* **2004**, *116*, 3972; *Angew. Chem., Int. Ed.* **2004**, *43*, 3882.

(4) (a) Rosenthal, U.; Burlakov, V. V.; Arndt, P.; Baumann, W.; Spannenberg, A. *Organometallics* **2005**, *24*, 456, and references therein. (b) Jemmis, E. D.; Phukan, A. K.; Jiao, H.; Rosenthal, U. *Organometallics* **2003**, *22*, 4958.

(5) (a) Pulst, S.; Arndt, P.; Heller, B.; Baumann, W.; Kempe, R.; Rosenthal, U. *Angew. Chem.* **1996**, *108*, 1175; *Angew. Chem., Int. Ed.* **1996**, *35*, 1112. (b) Bach, M. A.; Burlakov, V. V.; Arndt, P.; Baumann, W.; Spannenberg, A.; Rosenthal, U. *Organometallics* **2005**, *24*, 3047.

(6) (a) Pavan Kumar, P. N. V.; Jemmis, E. D. *J. Am. Chem. Soc.* **1988**, *110*, 125. (b) Jemmis, E. D.; Giju, K. T. *Angew. Chem.* **1997**, *109*, 633; *Angew. Chem., Int. Ed.* **1997**, *36*, 606. (c) Jemmis, E. D.; Parameswaran, P.; Phukan, A. K. *Mol. Phys.* **2005**, *103*, 897.

10.1021/om061030z CCC: $37.00

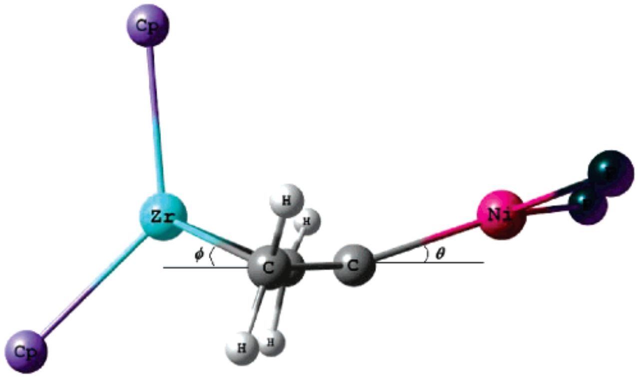

**Figure 1.** Schematic representation of the nonplanar geometry of $Cp_2Zr[\mu\text{-}(\eta^4{:}\eta^2\text{-}H_2C_4H_2)]NiL_2$ (L = $PPh_3$ and $PCy_3$). The groups attached to P are removed and the Cp rings are represented by a single atom for clarity. $\phi$ is the bending angle between the C4 plane and MC1C4 (ZrC1C4) plane, and $\theta$ is the bending angle between the C4 plane and M′C2C3 (NiC2C3) plane.

**Scheme 2**

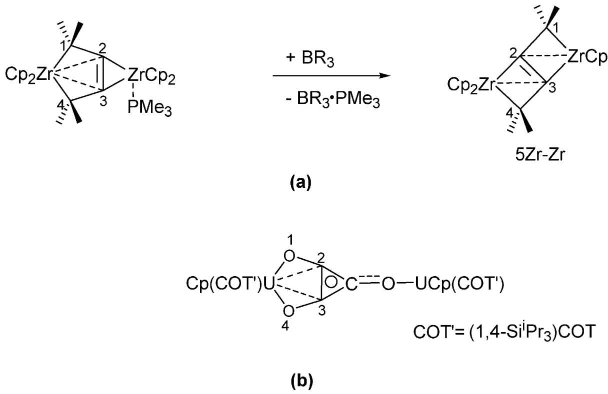

and co-workers reported[7a] a similar *cis*-type of complex, $Cp_2Zr[\mu\text{-}(\eta^4{:}\eta^2\text{-}H_2C_4H_2)]ZrCp_2(PMe_3)$, having a planar skeleton, where the $NiL_2$ fragment is replaced by the $ZrCp_2(PMe_3)$ fragment. The removal of donor ligand $PMe_3$ by a Lewis acid results in the well-known binuclear complex of *trans*-butatriene (**5Zr-Zr**, Scheme 2a).[7b] Summerscales et al. reported[8] a structurally similar uranium complex of cyclic-$C_3O_3^{2-}$ having a planar skeletal arrangement, Scheme 2b. These divergent experimental observations prompted us to study the reason for the nonplanarity of the nickel complex, **3M-M′**. We also probe the factors that control the preference of the homobimetallic zirconium complex for the *trans*-butatriene geometry (**5M-M′**), in contrast to the corresponding, so far only theoretically studied, *trans*-butadiyne Zr species (**6M-M′**).

## Computational Details

All structures were optimized using the hybrid HF-DFT method, B3LYP/LANL2DZ, based on Becke's three-parameter functional[9,10] including Hartree−Fock exchange contribution with a nonlocal correction for the exchange potential proposed by Becke[10a,b] together with the nonlocal correction for the correlation energy suggested by Lee et al.[10c] The LANL2DZ basis set uses the effective core potentials (ECP) of Hay and Wadt.[9,10] The nature of the stationary points is characterized by vibrational frequency calculations. The Gaussian 03 program package was used for all calculations.[11] The metallacyclopentynes and metallacyclocumulenes are given numbers, **1** and **2**, respectively (Scheme 1). The metal atom symbols are added after the number to indicate the structures calculated. Structures of the binuclear complexes are numbered by **3** and **4** and correspond to the complexes in which the ligands are *cis*-butatriene or *cis*-butadiyne. The letters **TS** are added along with the structure numbers to represent the transition state. Corresponding *trans* arrangements are given numbers **5** and **6**. Metal fragments involved are $Cp_2Zr$, $Cp_2Ti$, and $(PH_3)_2Ni$. Since there is a detailed study on *trans*-butadiyne complex **6**, this is not discussed in detail here.[6a,13]

Since the energy difference between **3M-M′** and its planar alternative **3-M-M′-TS** is less than 1 kcal/mol at the B3LYP/LANL2DZ level of theory, we have also optimized those structures at the BP86/ZORA/TZ2P level using the ADF05.01 package.[14] BP86 includes the exchange function of Becke[9,10a,b] and the correlation functional of Perdew.[9,15] The basis sets for all the atoms here are of triple-ζ quality, having two sets of polarization functions for all atoms. Zero-order regular approximation (ZORA) implemented in ADF05.01 is used to account for relativistic effects.[16] The structures obtained at the B3LYP/LANL2DZ level are used to obtain single-point energies at the MP2/LANL2DZ level to have a further check on the effect of electron correlation.[9] There is no major change in the geometry and the relative energies at different levels; the discussion is based on the results obtained at the B3LYP/LANL2DZ level unless otherwise specified.

## Results and Discussion

The discussion is arranged as follows. In order to understand the structure and bonding of these dimetallabicycles, a fragment approach, where the larger complex is constructed from the smaller distinct fragments, is used. Although the electronic structures of metallacyclopentynes (**1M**) and metallacyclocumulenes (**2M**) were studied previously,[4b,6,17] we begin with a brief description of them so that the binuclear complexes $Cp_2M[\mu\text{-}(\eta^4{:}\eta^2\text{-}H_2C_4H_2)]M'L_2$ and $Cp_2M[\mu\text{-}(\eta^4{:}\eta^2\text{-}HC_4H)]M'L_2$, where M = Zr and Ti and $M'L_2$ = $ZrCp_2$, $TiCp_2$, and $Ni(PH_3)_2$, could be easily understood. Several derivatives of metallacyclopentynes and metallacyclocumulenes are known experimentally.[4a] The parent structures are calculated to be minima on their potential energy surfaces. The variation of the electronic structures of **1M** and **2M** as a result of their interaction with the metal fragments are analyzed next, initially retaining a planar

---

[7] (a) Suzuki, N.; Aihara, N.; Takahara, H.; Watanabe, T.; Iwasaki, M.; Saburi, M.; Hashizume, D.; Chihara, T. *J. Am. Chem. Soc.* **2004**, *126*, 60. (b) Suzuki, N.; Watanabe, T.; Iwasaki, M.; Chihara, T. *Organometallics* **2005**, *24*, 2065.

[8] (a) Summerscales, O. T.; Cloke, F. G. N.; Hitchcock, P. B.; Green, J. C.; Hazari, N. *Science* **2006**, *311*, 829. (b) Summerscales, O. T.; Cloke, F. G. N.; Hitchcock, P. B.; Green, J. C.; Hazari, N. *J. Am. Chem. Soc.* **2006**, *128*, 9602.

[9] Hehre, W.; Radom, L.; Schleyer, P. v. R.; Pople, J. A. *Ab Initio Molecular Orbital Theory*; Wiley: New York, 1986.

[10] (a) Becke, A. D. *J. Chem. Phys.* **1993**, *98*, 5648. (b) Becke, A. D. *Phys. Rev. A* **1988**, *38*, 3098. (c) Lee, C.; Yang, W.; Parr, R. G. *Phys. Rev. B* **1988**, *37*, 785.

[11] (a) Hay, P. J.; Wadt, W. R. *J. Chem. Phys.* **1985**, *82*, 270. (b) Wadt, W. R.; Hay, P. J. *J. Chem. Phys.* **1985**, *82*, 284. (c) Hay, P. J.; Wadt, W. R. *J. Chem. Phys.* **1985**, *82*, 299.

[12] Frisch, M. J.; Pople, J. A.; et al. *Gaussian 03*, Revision C.02; Gaussian, Inc.: Wallingford, CT, 2004.

[13] Jemmis, E. D.; Giju, K. T. *J. Am. Chem. Soc.* **1998**, *120*, 6952.

[14] (a) *ADF2005.01*; SCM, Theoretical Chemistry, Vrije Universiteit: Amsterdam, The Netherlands, http://www.scm.com. (b) te Velde, G.; Bickelhaupt, F. M.; Baerends, E. J.; Fonseca Guerra, C.; van Gisbergen, S. J. A.; Snijders, J. G.; Ziegler, T. *J. Comput. Chem.* **2001**, *22*, 931. (c) Fonseca Guerra, C.; Snijders, J.; te Velde, G.; Baerends, E. J. *Theor. Chem. Acc.* **1998**, *99*, 391.

[15] Perdew, J. P. *Phys. Rev. B* **1986**, *33*, 8822.

[16] (a) Snijders, J. G.; Baerends, E. J. *Mol. Phys.* **1978**, *36*, 1789. (b) Snijders, J. G.; Baerends, E .J.; Ros, P. *Mol. Phys.* **1979**, *38*, 1909.

[17] (a) Jemmis, E. D.; Phukan, A. K.; Giju, K. T. *Organometallics* **2002**, *21*, 2254. (b) Lam, K. C.; Lin, Z. *Organometallics* **2003**, *22*, 3466. (c) Hashizume, D.; Suzuki, N.; Chihara, T. *Chem. Commun.* **2006**, 1233.

**Table 1. Bond Parameters (bond lengths in Å, bond angles in deg) and Wiberg Bond Indices (in *italics*) for Metallacyclopentynes and Metallacyclocumulenes[a]**

| molecule | M−C1 | M−C2 | C1−C2 | C2−C3 | C1−C2−C3 | M−C1−C2 |
|---|---|---|---|---|---|---|
| **1Zr** | 2.44 | 2.33 | 1.424 | 1.259 | 151.2 | 68.7 |
|  | (2.436)[17c] | (2.318) | (1.409) | (1.250) | (150.9) | (68.8) |
|  | *0.502* | *0.353* | *1.098* | *2.579* |  |  |
| **1Ti** | 2.385 | 2.229 | 1.406 | 1.266 | 151.9 | 66.3 |
|  | (2.353)[4c] | (2.202) | (1.393) | (1.248) | (151.7) | (66.4) |
|  | *0.633* | *0.401* | *1.139* | *2.516* |  |  |
| **2Zr** | 2.353 | 2.373 | 1.316 | 1.342 | 146.6 | 74.7 |
|  | (2.357)[4a] | (2.303) | (1.280) | (1.310) | (149.9) | (71.7) |
|  | *0.624* | *0.294* | *1.992* | *1.554* |  |  |
| **2Ti** | 2.242 | 2.259 | 1.302 | 1.344 | 145.1 | 73.9 |
|  | (2.210)[4a] | (2.252) | (1.277) | (1.338) | (147.6) | (70.3) |
|  | *0.663* | *0.338* | *2.047* | *1.467* |  |  |

[a] Experimental geometrical parameters are given in parentheses.[4a,c,17c]

**Table 2. Geometrical Parameters (bond lengths in Å and bond angles in deg) of the Dimetallabicycles (3M-M′ and 4M-M′) Calculated at the B3LYP/LANL2DZ Level of Theory[a]**

|  | bond lengths |  |  |  |  | bond angles |  |
|---|---|---|---|---|---|---|---|
| structure no. | C1−C2 | C2−C3 | M−C1 | M−C2 | M′−C2 | C1−C2−C3 | C2−M′−C3 |
| **3Zr-Ni** | 1.459 | 1.340 | 2.366 | 2.438 | 1.927 | 142.2 | 40.7 |
|  | (1.452)[5b] | (1.305) | (2.323) | (2.397) | (1.908) | (139.0) | (39.7) |
| **3Ti-Ni** | 1.445 | 1.335 | 2.251 | 2.336 | 1.928 | 141.0 | 40.5 |
| **3Zr-Zr** | 1.491 | 1.375 | 2.307 | 2.566 | 2.203 | 135.8 | 36.4 |
| **3Ti-Ti** | 1.471 | 1.344 | 2.199 | 2.445 | 2.069 | 136.6 | 37.9 |
| **4Zr-Ni** | 1.346 | 1.450 | 2.248 | 2.480 | 1.910 | 137.2 | 44.6 |
|  | (1.322)[5a] | (1.410) | (2.239) | (2.389) | (1.911) | (139.4) | (43.1) |
| **4Ti-Ni** | 1.335 | 1.449 | 2.109 | 2.380 | 1.909 | 134.1 | 44.6 |
|  | (1.333)[5a] | (1.419) | (2.118) | (2.340) | (1.907) | (133.3) | (40.6) |
| **4Zr-Zr** | 1.355 | 1.540 | 2.223 | 2.584 | 2.211 | 132.1 | 40.8 |
| **4Ti-Ti** | 1.342 | 1.499 | 2.095 | 2.476 | 2.067 | 130.2 | 42.5 |

[a] Experimental values for specific structures are given in parentheses.[5] First and second metal symbols in the structure number correspond to $\eta^4$- and $\eta^2$-coordination, respectively.

**Table 3. Bending Angles and the Energy Barriers ($E_{3-\mathrm{TS}}$)[a] between Planar (3M-M′-TS) and Bent Geometries (3M-M′) of Dimetallabicycles at B3LYP/LANL2DZ, BP86/ZORA/TZP, and MP2/LANL2DZ**

|  |  | B3LYP/LANL2DZ |  |  | BP86/ZORA/TZP |  |  | MP2/LANL2DZ[c] |
|---|---|---|---|---|---|---|---|---|
| structure no. | bent (**3M-M′**) | planar (**3M-M′-TS**) | $\theta^b$ | $\phi^b$ | planar (**3M-M′-TS**) | $\theta^b$ | $\phi^b$ | planar (**3M-M′-TS**) |
| **3Zr-Ni** | 0.0 | 0.8 | 20.3 | 17.1 | 1.31 | 21.4 | 17.0 | 0.9 |
| **3Ti-Ni** | 0.0 | 0.76 | 19.3 | 14.8 | 1.45 | 21.7 | 14.3 | 2.6 |
| **3Zr-Zr** | 0.0 | 0.72 | 0.8 | 16.0 | 0.44 | 0.3 | 17.2 | 1.1 |
| **3Ti-Ti** | 0.0 | 0.08 | 2.1 | 5.7 | 0.8 | 2.4 | 5.9 | 0.4 |

[a] The energy difference between the planar (**3M-M′-TS**) and bent (**3M-M′**) geometries of dimetallabicycles. [b]The bending angle, $\phi$, is the angle between the C4 and MC1C4 planes, and $\theta$ is the angle between the C4 and M′C2C3 planes. [c]Single-point calculation at the geometry obtained at B3LYP/LANL2DZ.

geometry. A correlation diagram between the planar and bent geometries is then constructed to understand the factors that control the out-of-plane distortion of the $Cp_2M$ and the $M'L_2$ fragment. The energetics of the *cis* and *trans* arrangement for **3M-M′** and **5M-M′** are discussed in the end.

**Metallacyclopentynes (1M) and Metallacyclocumulenes (2M).** The theoretical and experimental geometrical parameters of the metallacyclopentynes (**1M**) and the metallacyclocumulenes (**2M**) are given in Table 1. Both the metallacyclopentynes (**1M**) and metallacyclocumulenes (**2M**) have a planar skeleton and the calculated geometrical parameters are close to the experimentally reported values.[4,17] The M−C2 bond distances in metallacyclopentynes are shorter than the M−C1 bond distances. In comparison with 2-butyne (1.473 and 1.219 Å), the C1−C2 distances of **1Zr** (1.424 Å) and **1Ti** (1.406 Å) are shorter, while the C2−C3 triple bonds of **1Zr** (1.259 Å) and **1Ti** (1.266 Å) are longer. This confirms the delocalized nature of the $C_4$ fragment and the greater $\pi$-delocalization to the C2−C3 region. There are longer C2−C3 and shorter C1−C2 bond distances in metallacyclocumulenes than in metallacyclopentynes (Table 1). The Wiberg bond index[18] at the C2−C3 bond shows a delocalized triple bond in metallacyclopentyne and a delocalized double bond in the metallacyclocumulene. The smaller titanium atom can come closer to both of the $C_4$ fragments than the zirconium. This results in more effective overlap of titanium with the central C2−C3 bond. Therefore, M−C1 bond distances are shorter and C2−C3 is longer for **1Ti** than for **1Zr**.

The important molecular orbitals of **1M** and **2M** are shown in Figure 2. The HOMO and HOMO-3 of **1M** correspond to the interaction of the in-plane $\pi$-orbitals with the metal orbitals. HOMO-2 is mainly a $\pi$-orbital on the C2−C3 bond and does not have any significant interaction with the metal. The frontier molecular orbitals of the metallacyclopentyne on the side of $C_4$ and away from the metal and the perpendicular $\pi$-MOs are ideally suited for further reactions. The nature of the interaction of the in-plane $\pi$-orbitals with the metal orbital is similar in

---

(18) (a) Reed, A. E.; Weinstock, R. B.; Weinhold, F. *J. Chem. Phys.* **1985**, *83*, 735. (b) Reed, A. E.; Weinhold, F. *J. Chem. Phys.* **1985**, *83*, 1736. (c) Reed, A. E.; Curtiss, L. A.; Weinhold, F. *Chem. Rev.* **1988**, *88*, 899.

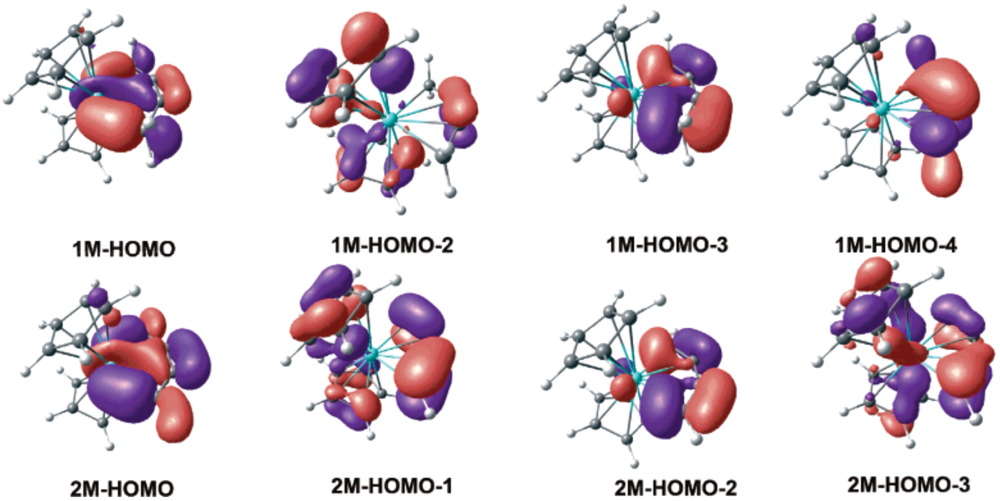

**Figure 2.** Important molecular orbitals of metallacyclopentyne (**1M**) and metallacyclocumulene (**2M**).

both metallacyclopentyne and metallacyclocumulene. However, the perpendicular $\pi$-orbitals are mainly localized on C2 and C3 carbon atoms (1M-HOMO-2) in metallacyclopentyne. It has also some contribution from the $CH_2$ group orbitals at C1 and C4 (1M-HOMO-4). Hence these perpendicular $\pi$-orbitals in metallacyclopentyne are available for further interaction with the second metal. The perpendicular $\pi$-orbital in metallacyclocumulene are more delocalized (2M-HOMO-1 and 2M-HOMO-3) and less available for further interaction with the second metal. Hence the frontier molecular orbitals in metallacyclopentyne are the in-plane and perpendicular $\pi$-orbitals at C2−C3. There is only the in-plane molecular orbital available in metallacyclocumulene.[4b,6b]

**Dimetallabicycles.** The structure and bonding of bimetallic, *cis*-bridged $Cp_2M(\mu\text{-}\eta^4\text{:}\eta^2\text{-}H_2C_4H_2)M'L_2$ (**3M-M′**),[5b,7a] where M = Zr and Ti and $M'L_2$ = $ZrCp_2$, $TiCp_2$, and $Ni(PH_3)_2$, are compared here with the corresponding cumulenic complexes (**4M-M′**), Table 2.[5a,19] The complexes **3M-M′** are synthesized only with M = Zr and M′ = Ni. Examples of complexes (**4M-M′**) having M = Zr, Ti and M′ = Ni are also isolated. No examples of the *cis*-bridged homobimetallic compounds **3Ti-Ti** and **4Zr-Zr** are known experimentally so far. We had shown earlier that cumulenic complexes are more stable for M′ = Ni than for M′ = Zr and Ti.[6b] Both C1−C2 and C2−C3 bonds are elongated in **3M-M′** and **4M-M′**. In both cases, the magnitude of elongation is in the order $M'L_2 = ZrCp_2 > TiCp_2 > Ni(PH_3)_2$. This is in accordance with the diffuseness of the metal orbitals. As a result of the interaction of the second metal with the C2−C3 bond, the M−C2 bond is elongated in comparison to the parent metallacycles (Table 2). The $MC_4M'$ skeleton in **3M-M′** is nonplanar, in contrast to the planar geometry in **4M-M′**.

The planar alternative to **3M-M′** is a transition state (**3M-M′-TS**) for the interconversion of the two possible bent geometries, and its barrier for interconversion ($E_{3-TS}$) is less than 1 kcal/mol (Table 3). Since the barriers are very low, we computed the values at several levels of theory. All the results show that the energies for the interconversion are very low. A low-energy barrier is reported for the inversion of the pyramidal boron in cyclic-$(CH_2)(SiH_2)BH$ via a planar geometry to the equivalent pyramidal geometry[20a] and for the inversion of bridging and terminal hydrogens via planar geometry in several three-membered rings of the group 13 elements.[20b,c] The $M'L_2$ and $Cp_2M$ fragments have deviation from the C4 plane. The bending angle, $\phi$, defined as the angle between the C4 and MC1C4 plane, is maximum for **3Zr-Ni** (20.3°) and minimum for **3Zr-Zr** (0.8°). Similarly, the bending angle, $\theta$, defined as the angle between the C4 and M′C2C3 plane, is maximum for **3Zr-Ni** (17.1°) and minimum for **3Ti-Ti** (5.7°). It is interesting to note that the bending angle, $\phi$, is close to zero for homodimetallabicycles (**3Zr-Zr** and **3Ti-Ti**). Corresponding angles in our experimental binuclear complexes, $Cp_2Zr[\mu\text{-}(\eta^4\text{:}\eta^2\text{-}H_2C_4H_2)]NiL_2$ (L = $PPh_3$, $PCy_3$), are $\phi = 16.5°$ and $\theta = 16.9°$ for L = $PPh_3$ and $\phi = 5.7°$ and $\theta = 12.3°$ for L = $PCy_3$.[5b] The phosphine ligands are nearly in the C2−Ni−C3 plane. The deviation of the calculated angle (6°) between the planes PNiP and C2NiC3 is only 1° from the X-ray data (5°) for both molecules. Our calculated values at the B3LYP/LANL2DZ level of theory for the experimentally reported structures (**3M-M′**) with the same substituents are $\phi = 17.7°$ and $\theta = 18.4°$ for L = $PPh_3$ and $\phi = 9.1°$ and $\theta = 7.9°$ for $PCy_3$.

The bonding in the planar alternatives (**3Zr-Zr-TS** and **3Ti-Ti-TS**) of **3Zr-Zr** and **3Ti-Ti** is best described by treating the bridging ligand as formally a *cis*-$[H_2CCCCH_2]^{(-4)}$ species, making both the metals in the formal +4 oxidation state. This leads to 10 valence electrons in the $\pi$-frame. The C2−C3 $\pi$-bond perpendicular to the $MC_4M'$ plane does not interact substantially with the metals. The remaining eight $\pi$-type valence electrons of the $[H_2CCCCH_2]^{(-4)}$ ligand occupy four in-plane delocalized orbitals resulting from the interaction with the $Cp_2M$ fragment orbitals. The bonding here is very similar to that in the *cis*-cumulene complexes **4Zr-Zr** and **4Ti-Ti** except that **3Zr-Zr** and **3Ti-Ti** have an ethylenic $\pi$-bond in place of the *cis*-butadiene of the butadiyne complex. Nickel complexes **3Zr-Ni** and **3Ti-Ni** are described as formed by the interaction of *cis*-$[H_2CCCCH_2]^{(-4)}$ and metal M as (+4) and nickel as Ni(2+).

In order to understand the factors for the nonplanarity, we have used a correlation diagram connecting important molecular orbitals of the planar (**3Zr-Ni-TS**), the half-bent structure, and

---

[19] Rosenthal, U.; Pellny, P.-M.; Kirchbauer, F. G.; Burlakov, V. V. *Acc. Chem. Res.* **2000**, *33*, 119.

[20] (a) Giju, K. T.; Phukan, A. K.; Jemmis, E. D. *Angew. Chem.* **2003**, *115*, 557; *Angew. Chem., Int. Ed.* **2003**, *42*, 539. (b) Srinivas, G. N.; Anoop, A.; Jemmis, E. D.; Hamilton, T. P.; Lammertsma, K.; Leszczynski, J.; Schaefer, H. F., III. *J. Am. Chem. Soc.* **2003**, *125*, 16397. (c) Jemmis, E. D.; Parameswaran, P. *Chem.−Eur. J.* **2007**, *13*, 2622.

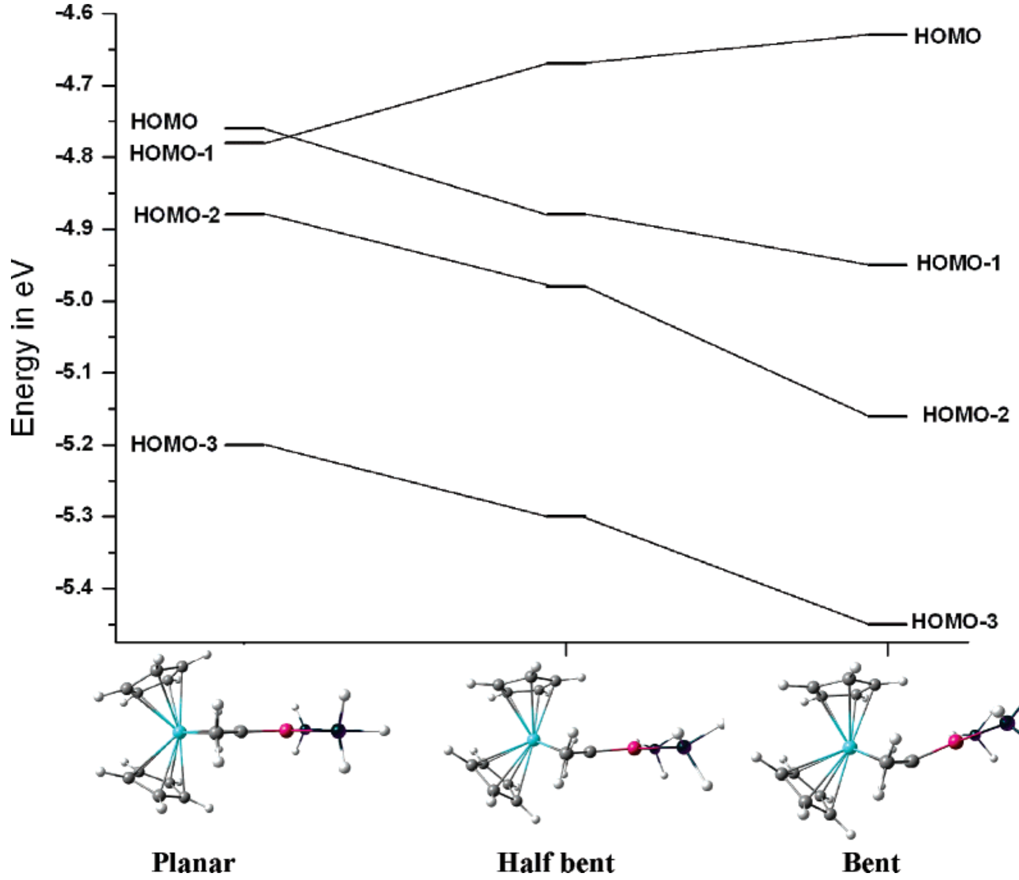

**Figure 3.** Correlation diagram connecting important molecular orbitals of planar (**3Zr-Ni-TS**), half-bent structure, and bent (**3Zr-Ni**) geometries of $Cp_2Zr[\mu\text{-}(\eta^4{:}\eta^2\text{-}H_2C_4H_2)]Ni(PH_3)_2$ at the B3LYP/LANL2DZ level of theory. The planar (**3Zr-Ni-TS**) and bent (**3Zr-Ni)** geometries are transition state and minimum on the potential energy surface. The half-bent structure is an intermediate structure in which $Cp_2Zr$ has a deviation from the C4 plane similar to the bent structure **3Zr-Ni**, while the $Ni(PH_3)_2$ is in the C4 plane similar to the planar structure **3Zr-Ni-TS**. The corresponding molecular orbitals for planar and bent geometries are shown in Figure 4.

perfectly bent structure (**3Zr-Ni**) (Figure 3). The planar structure (**3Zr-Ni-TS**) is a transition state and the bent (**3Zr-Ni**) geometry is a minimum on the potential energy surface. The half-bent structure is an intermediate structure (single-point calculation) in which $Cp_2Zr$ deviates from the C4 plane similar to the bent structure, **3Zr-Ni**, while the $Ni(PH_3)_2$ is in the C4 plane similar to the planar structure, **3Zr-Ni-TS**. A similar interaction diagram is obtained for **3Ti-Ni** as well. The HOMO of the planar structure is antibonding between the $\pi$-orbitals located on C2 and C3 and the d-orbital on the nickel (Figure 4a). This is similar to the HOMO of the nickel acetylene (Figure 4d) complex, which has an antibonding interaction between the $\pi$-MO and the d-orbital on nickel. The HOMO-1 also has a slight antibonding interaction between the in-plane $\pi$-orbitals and the d-orbital on nickel. As a result of the out-of-plane bending, these perpendicular $\pi$-MOs undergo mixing, and two new perpendicular $\pi$-MOs result (Figure 4b). One of them is stabilized by the bonding interaction with the d-orbital on nickel (HOMO-1), leading to the elongation of the C2−C3 bond length (1.33 Å to 1.34 Å). The other one (HOMO) is destabilized as a result of the more antibonding interaction between C1 and C2, which is reflected in the elongated bond distance. However, the antibonding interaction between Ni and C2−C3 $\pi$-MO is less here in comparison to that in the planar structure. This mainly results in the bending of the $Ni(PH_3)_2$ fragment from the C4 plane. The HOMO-2 and HOMO-3 are also more stabilized in the puckered structure in comparison to the planar structure. The bending of $Cp_2M$ from the C4 plane allows the rehybridization of the in-plane p-orbitals of C1 and C2, and as a result it reduces the antibonding interaction between C1 and C2 and between C3 and C4 (HOMO-2 and HOMO-3). The need of reorganization to get effective overlap is more for $Cp_2Zr$ than that of $Cp_2Ti$, and as a result the bending angle, $\phi$, for **3Zr-M′** is more. The bending of the $Ni(PH_3)_2$ group reduces the antibonding interaction between nickel orbitals and the $\pi$-MO at the C2−C3 bond, whereas the bending of $Cp_2M$ mainly reduces the antibonding interaction between C1 and C2. A similar nonplanarity is reported for the hydrocarbon analogues of these bicyclic compounds,[21a,b] cyclobutadiene dication, and $L_2W(\mu\text{-}CR)_2WL_2$ (L = H, Me, F, OH; R = H, F, Me).[21c−f] The nonplanarity of the cyclobutadiene dication releases the antibonding (1,3) $\sigma$-interactions, while that of $L_2W(\mu\text{-}CR)_2WL_2$ is mainly due to the stabilization of the metal−metal $\sigma$-bond.

There is no MO in the frontier range of **3Ti-Ti** and **3Zr-Zr** corresponding to the HOMO and HOMO-1 of the nickel complex. There is however a vacant d-orbital ($d_{z^2}$) on M′ in the $C_4$ plane of the molecule (Figure 4c). The reasons for the stabilization of the HOMO-2 and HOMO-3 in **3Ti-Ti** and **3Zr-Zr** are similar to those of **3Zr-Ni**.

The stability of these complexes can be analyzed from the isodesmic eqs 1 and 2. The optimum C−C−H bond angles for the formation of $C_2H_2Ni(PH_3)_2$, $C_2H_2TiCp_2$, and $C_2H_2ZrCp_2$ are 147.3°, 139.6°, and 133.3° respectively (Table 4). These variations of the CCH bond angle depend on the size of the metal. The larger the size of the metal atom, the smaller will be the CCH bond angle so as to result in a large effective span

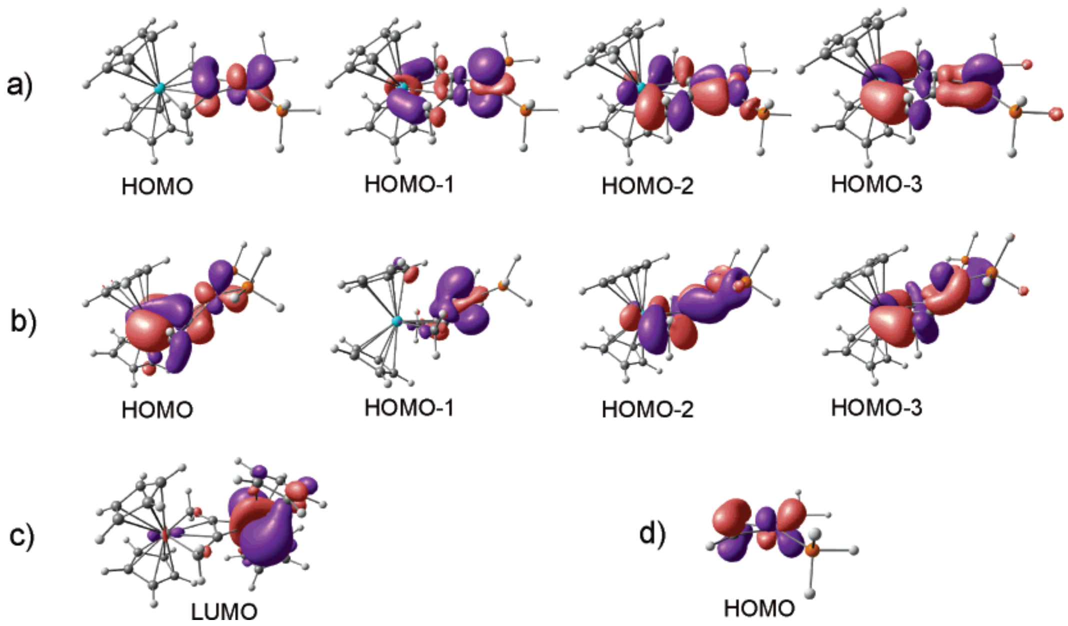

**Figure 4.** Important molecular orbitals of (a) planar, (b) bent geometries of **3Zr-Ni** and (c) LUMO of **3Zr-Zr**, and (d) HOMO of the nickel acetylene complex.

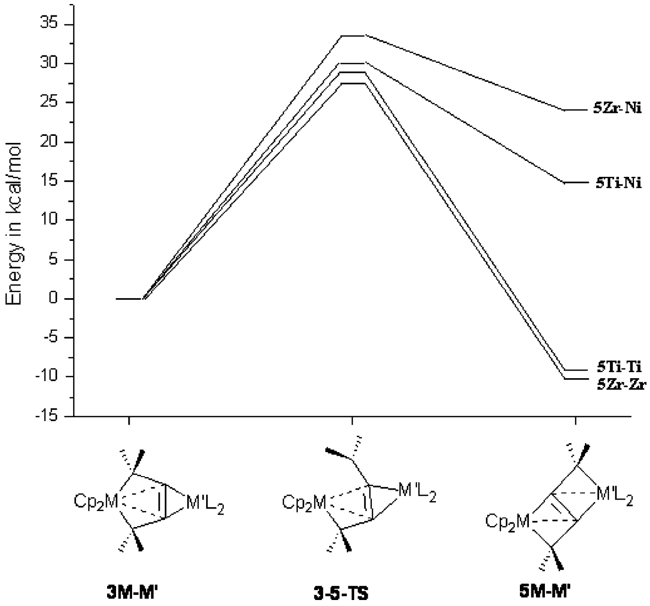

**Figure 5.** Potential energy diagram for the interconversion of *cis* (**3M-M′**) to *trans* (**5M-M′**) dimetallabicycles of metallacyclopentyne. **3-5-TS** is the transition state for their interconversion.

for the $\pi$-orbital and thereby better overlap with the metal. Hence, the larger zirconium atom requires a smaller CCH bond angle (larger bending away from the metal M) to have an effective interaction in comparison to the smaller nickel atom. As a result, the complexes are more stable when the CCH bond angles of the metal acetylene complexes are closer to the C1−C2−C3 bond angle of the metallacyclopentyne.

The exothermicity for the metallacyclocumulenes indicates the greater stability of the bimetallic complexes of metallacyclocumulenes in comparison to those of the metallacyclopentynes. The energies obtained from the isodesmic eq 1 show that the formation of the complexes **4M-Ni** is more favorable than that of the complexes **3M-Ni**. It is clear from Table 4 that when the C−C−H bond angle in M′L$_2$ is closer to the C1−C2−C3 angle of **1M**, the stability of the complex will be greater. As the bond angles of C1−C2−C3 and C−C−H become closer to each other, the strain involved in the formation of the binuclear complex **4M-Ni** will be less and hence they are more exothermic. The strain is proportional to the magnitude of deviation of the C1−C2−C3 bond angle from the C−C−H bond angle. The closer the C1−C2−C3 bond angle is to the C−C−H bond angle, the more the strain in **3M-Ni** is reduced. This allows the relatively unhybridized $\pi$-MO in the orthogonal plane to mix with the in-plane $\pi$-MO. Even though the span of the hybridized $\pi$-MO is reduced by this mixing, it is helpful to reduce the antibonding interaction between the Ni orbital and $\pi$-MO at the C2−C3 bond. The need for more reorganization is less when the Ni(PH$_3$)$_2$ fragment is replaced by M′ Cp$_2$, so that the out-of-plane bending is less. A puckered geometry might give an easier opening for another metal to approach the butatriene fragments and trigger the reaction.

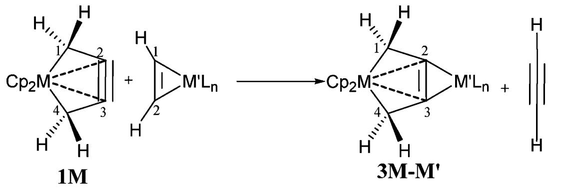

(1)

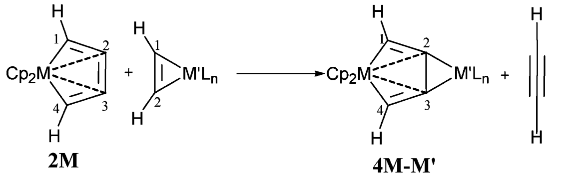

(2)

Experimentally the *cis* complex **3Zr-Ni** is obtained by the interaction of metallacyclopentyne with nickel olefin complexes. The calculated reaction energies for these complexes are exothermic for **3Ti-Ni** (−2.3 kcal/mol) and **3Zr-Ni** (−3.9 kcal/mol) and endothermic for **3Zr-Zr** (10.3 kcal/mol) and **3Ti-Ti** (9.3 kcal/mol). This explains the experimental realization of **3Zr-Ni** complexes. Similarly, the exothermicity for **3Ti-Ni** complex is a good indication that this is a realistic experimental target. However, similar experimental attempts to synthesize **3Ti-Ni**

**Table 4. Reaction Energies, ΔE (kcal/mol), Obtained From Isodesmic Eqs 1 and 2[a]**

| | **1Zr** | **1Ti** | **2Zr** | **2Ti** | **3Zr-Ni** | **3Ti-Ni** | **3Zr-Zr** | **3Ti-Ti** | **4Zr-Ni** | **4Ti-Ni** | **4Zr-Zr** | **4Ti-Ti** |
|---|---|---|---|---|---|---|---|---|---|---|---|---|
| C1−C2−C3 angle | 151.2 | 151.9 | 146.6 | 144.1 | 142.2 | 141.0 | 135.8 | 136.6 | 137.2 | 134.1 | 132.1 | 130.2 |
| $\Delta E$ | | | | | 1.2 | 2.8 | 10.7 | 7.9 | −9.3 | −9.1 | −1.8 | −6.0 |
| $\Delta E_{3-5}$[b] | | | | | 24.1 | 14.8 | −10.3 | −9.1 | | | | |
| $\Delta Ea_{3-5}$[c] | | | | | 33.6 | 30.1 | 27.4 | 28.1 | | | | |

[a] C−C−H is the angle of $C_2H_2Ni(PH_3)_2$, $C_2H_2TiCp_2$, and $C_2H_2ZrCp_2$, which are 147.3°, 139.6°, and 133.3°, respectively. [b,c] $\Delta E_{3-5}$ and $\Delta Ea_{3-5}$ are the energy difference and its barrier for the interconversion of **3M-M′** and **5M-M′**, respectively.

**Table 5. Geometrical Parameters (bond lengths in Å and bond angles in deg) of the Dimetallabicycles (5M-M′) Calculated at the B3LYP/LANL2DZ Level of Theory[a]**

| | bond lengths | | | | | | | bond angles | |
|---|---|---|---|---|---|---|---|---|---|
| molecule | C1−C2 | C2−C3 | C3−C4 | M−C1 | M−C3 | M′−C2 | M′−C4 | MC3C2M′ | C1C2C3 |
| **5Zr-Ni** | 1.518 | 1.395 | 1.502 | 2.275 | 2.158 | 1.952 | 1.980 | 166.6 | 129.0 |
| **5Ti-Ni** | 1.495 | 1.398 | 1.462 | 2.150 | 2.032 | 1.977 | 2.011 | 141.5 | 126.6 |
| **5Zr-Zr** | 1.530 | 1.389 | 1.523 | 2.236 | 2.218 | 2.218 | 2.236 | 177.5 | 127.1 |
| | (1.492)[7b] | (1.371) | (1.492) | (2.225) | (2.184) | (2.184) | (2.225) | (180.0) | (129.9) |
| **5Ti-Ti** | 1.503 | 1.370 | 1.503 | 2.113 | 2.073 | 2.073 | 2.113 | 179.9 | 126.0 |
| | (1.443)[7c] | (1.325) | (1.443) | (2.152) | (2.268) | (2.268) | (2.152) | (180.0) | (131.7) |

[a] Experimental values for specific structures are given in parentheses.[7b,23]

lead to the formation of **5Ti-Ti**, as seen from NMR analysis.[4b] Suzuki and co-workers reported the zirconium complex of zirconacyclopentyne of $Cp_2Zr[(\mu\text{-}\eta^4{:}\eta^2\text{-}H_2C_4H_2)]ZrCp_2(PMe_3)$ as a ligand-stabilized example of **3Zr-Zr**, having a flat geometry.[7a] The calculated structure of $Cp_2Zr[(\mu\text{-}\eta^4{:}\eta^2\text{-}H_2C_4H_2)]ZrCp_2(PMe_3)$ shows a different behavior. Here, the metals are not in the same plane with the $C_4$ skeleton and the bending angles are $\phi = 11.9°$ and $\theta = 0.9°$ at the B3LYP/LANL2Z level of theory and $\phi = 13.2°$ and $\theta = 0.8°$ at the BP86/ZORA/TZ2P level of theory. The optimization of the planar structure converges into the nonplanar geometry. The CCH angle in $Cp_2Zr(PMe_3)C_2H_2$ is 136.4°, which is higher than that of $Cp_2ZrC_2H_2$ (133.3°). The calculated angle C1−C2−C3 of $Cp_2Zr[(\mu\text{-}\eta^4{:}\eta^2\text{-}H_2C_4H_2)]ZrCp_2(PMe_3)$ (138.4°) is close to that of the X-ray data (139.1°). The planarity of $Cp_2Zr[(\mu\text{-}\eta^4{:}\eta^2\text{-}H_2C_4H_2)]ZrCp_2(PMe_3)$ may be due to the packing effect in the solid phase of the single crystal. Similar structural alteration is observed for the complex $[(Me_3SiCH_2)_2W(\mu\text{-}CSiMe_3)]_2$.[21] The X-ray structure of this tungsten complex shows a planar geometry, while the *ab initio* calculations predict a nonplanar geometry similar to that of the cyclobutadiene dication.[22] The removal of the $PMe_3$ group by a Lewis acid gave a *trans* geometry as a minimum (**5Zr-Zr**). There is no report on the experimental structure of **3Ti-Ti**, but experiments to realize the **3Ti-Ti** complex result in the *trans* geometry (**5Ti-Ti**). We have recently synthesized this *trans* bimetallic complex (**5Ti-Ti**) by the reaction of titanacyclopentyne with the titanocene complex of bistrimethylsilylacetylene in THF.[23]

**Energetics of *cis*−*trans* Isomerization.** The relative energies ($\Delta E_{3-5}$) between *cis* (**3M-M′**) and *trans* (**5M-M′**) geometries and corresponding barriers ($\Delta Ea_{3-5}$) for their interconversion are given in Table 4. The geometrical parameters of **5M-M′** are shown in Table 5. The relative energies show that the *cis* geometries (**3Ti-Ni** and **3Zr-Ni**) are more stable when $L_2M' = (PH_3)_2Ni$. In contrast, the *trans* geometries (**5Ti-Ti** and **5Zr-Zr**) are more preferred when $L_2M' = Cp_2Zr$ and $Cp_2Ti$ (Figure 5). The nickel fragment $(PH_3)_2Ni$ in **5Ti-Ni** and **5Zr-Ni** is not in the plane MC2C3, just as observed in the *cis* complexes. The bending angles (the angle between M′C2C3 and MC2C3) in **5Zr-Ni** and **5Ti-Ni** are 13.4° and 38.5°. On the other hand, both **5Ti-Ti** and **5Zr-Zr** have almost planar $MC_4M'$ skeletons.

In comparison to **3M-M′**, the C1−C2 and C2−C3 bond lengths are more elongated in **5M-M′**. The elongation of the C2−C3 bond length is more when $M'L_2 = Ni(PH_3)_2$. The bonding in **5M-M′** is similar to that in **3M-M′** except that the bridging ligand should be considered as formally a *trans*-butatriene. Similar to the *cis* complexes, the antibonding interaction between the π-MO at the C2−C3 bond and the nickel explains the deviation from planarity. The greater preference for the four-membered over the three-membered ring reduces the angle of deviation of **5Zr-Zr** and **5Ti-Ti** from planarity in comparison to **3Zr-Zr** and **3Ti-Ti**.

The LUMOs of **3Ti-Ti** and **3Zr-Zr** have d-orbitals on M′ parallel to the MC4 plane of the molecule (Figure 4c). It can accept electrons from Lewis bases such as $PMe_3$ and THF and stabilize the planar structure. As a result, the two Cp rings are twisted toward one side from the pseudo-tetrahedral geometry. This explains the experimental observation of the planar geometry of $Cp_2Zr[(\mu\text{-}\eta^4\text{-}H_2C_4H_2)]ZrCp_2(PMe_3)$. The lesser preference for higher coordination of the smaller titanium atom precludes the formation of a similar structure. The vacant orbital on Zr and Ti can form a σ-bond with one of the terminal carbon atoms (C1 or C4) and results in the *trans* geometry. For this process, another M−C bond needs to be cleaved, and hence the barrier for this transformation is very high (Figure 5).

Hessen and co-workers reported[24] the formation of $Cp^*_2Ti(Cl)[\mu\text{-}(\eta^3{:}\eta^3\text{-}RNCCNR)]Ti(Cl)Cp^*_2$ containing the heterocumulenic RN═C═C═NR with NCCN skeleton in a *trans* geometry. Lentz and co-workers reported[25] a similar molybdenum complex with the NCCN skeleton in a *cis* geometry. In view of the variety of structures and varying energetics observed

---

(21) (a) Wagner, H. U.; Szeimies, G.; Chandrasekhar, J.; Schleyer, P. v. R.; Pople, J. A.; Binkley, J. S. *J. Am. Chem. Soc.* **1978**, *100*, 1210. (b) Wiberg, K. B.; Bonneville, G. *Tetrahedron Lett.* **1982**, *23*, 5385. (c) Andersen, R. A.; Galyer, A. L.; Wilkinson, G. *Angew. Chem.* **1976**, *88*, 692; *Angew. Chem., Int. Ed. Engl.* **1976**, *15*, 609. (d) Chisholm, M. H.; Cotton, F. A.; Extine, M.; Murrilo, C. A. *Inorg. Chem.* **1978**, *17*, 696. (e) Cotton, F. A.; Schwotzer, W.; Shamshoum, E. S. *Organometallics* **1983**, *2*, 1167. (f) Chisholm, M. H.; Huffman, J. C.; Heppert, J. A. *J. Am. Chem. Soc.* **1985**, *107*, 5116.

(22) Jemmis, E. D.; Giju, K. T. *Organometallics* **1997**, *16*, 1425.

(23) Burlakov, V. V.; Arndt, P.; Baumann, W.; Spannenberg, A.; Rosenthal, U.; Parameswaran, P.; Jemmis, E. D. *Chem. Commun.* **2004**, 2074.

(24) Hessen, B.; Blenkers, J.; Teuben, J. H.; Helgesson, G.; Jagner, S. *Organometallics* **1989**, *8*, 830.

(25) Lentz, D.; Brüdgam, I.; Hartl, H. *Angew. Chem.* **1984**, *96*, 511; *Angew. Chem., Int. Ed. Engl.* **1984**, *23*, 525.

in the current study, further experimental investigations are expected in this area.[26]

## Conclusions

We have investigated the structure and bonding in the *cis* and *trans* dimetallabicycles starting from metallacyclopentynes and compared them with the binuclear complexes from metallacyclocumulenes. The *cis* dimetallabicycles of the metallacyclopentynes are not planar in comparison to the *cis* complexes of metallacyclocumulenes. The bending angle of $M'L_2$, $\theta$, for **3Ti-Ni** and **3Zr-Ni** has a large value, while that of **3Ti-Ti** and **3Zr-Zr** is close to zero. This nonplanarity of the nickel complex is an attempt to reduce the antibonding interaction between the nickel d-orbital and the perpendicular $\pi$-MO at the C2−C3 bond. The out-of-plane bending of $Cp_2M$ ($\phi$) reduces the antibonding interaction between C1 and C2. The calculated reaction energies for these complexes show that the nickel complexes **3Ti-Ni** and **3Zr-Ni** are more stable than the homodimetallabicycles, **3Zr-Zr** and **3Ti-Ti**. The vacant d-orbital of titanium and zirconium leads to the instability of the *cis* complexes. It can be stabilized by an electron-donating group or by the interaction with the C1 (or C4) carbon atom to form *trans* complexes. The experimental observation of the flat $Cp_2Zr[\mu\text{-}(\eta^4:\eta^2\text{-}H_2C_4H_2)]ZrCp_2(PMe_3)$ and *trans* geometry of the $Cp_2Ti[\mu\text{-}(\eta^3:\eta^3\text{-}H_2C_4H_2)]TiCp_2$ and $Cp_2Zr[\mu\text{-}(\eta^3:\eta^3\text{-}H_2C_4H_2)]ZrCp_2$ supports this analysis. The lesser preference for higher coordination numbers at the smaller titanium atom prevents the experimental realization of *cis* complexes of **3Ti-Ti** with an electron-donating group such as $PMe_3$.

**Acknowledgment.** We thank the Indo-German DST-DAAD project based personnel exchange program for financial support. The Supercomputer Education and Research Centre, IISc, provided computational facilities.

**Supporting Information Available:** Cartesian coordinates and total energies of all the molecules are available free of charge via the Internet at http://pubs.acs.org.

OM061030Z

---

[26] Rosenthal, U.; Burlakov, V. V.; Bach, M. A.; Beweries, T. *Chem. Soc. Rev.*, in press (DOI: 10.1039/b605734a).